ARTICLES
https://doi.org/10.1038/s41559-019-0944-9
nature ecology & evolution

Privatization of public goods can cause population decline

Richard J. Lindsay, Bogna J. Pawlowska and Ivana Gudelj*

Microbes commonly deploy a risky strategy to acquire nutrients from their environment, involving the production of costly public goods that can be exploited by neighbouring individuals. Why engage in such a strategy when an exploitation-free alternative is readily available whereby public goods are kept private? We address this by examining metabolism of *Saccharomyces cerevisiae* in its native form and by creating a new three-strain synthetic community deploying different strategies of sucrose metabolism. Public-metabolizers digest resources externally, private-metabolizers internalize resources before digestion, and cheats avoid the metabolic costs of digestion but exploit external products generated by competitors. A combination of mathematical modelling and ecological experiments reveal that private-metabolizers invade and take over an otherwise stable community of public-metabolizers and cheats. However, owing to the reduced growth rate of private-metabolizers and population bottlenecks that are frequently associated with microbial communities, privatizing public goods can become unsustainable, leading to population decline.

A common feeding strategy deployed by microorganisms involves secretion of metabolic products into the external environment to break down or capture nutrients[1–9]. Although this strategy has enabled microbes to successfully adopt diverse lifestyles from free living to symbiotic and pathogenic[7,8], it is seemingly flawed. External digestion can prevent successful proliferation in low density or low resource environments because metabolic products can be lost into the environment[10–12]. The secreted metabolic products can thus be regarded as cooperative public goods—they are costly to produce and benefit every individual in the shared environment. The fitness potential of producers is therefore also limited by the fact that public goods can be exploited by non-producing cheats who do not contribute to the cost of their production, but still reap the rewards. This gives cheats an advantage that can drive a decline of public goods producers[2–5,13–15].

Numerous mechanisms can enable producers to limit the loss of public goods, such as having preferential access to the public goods[2,4,14,16], coupling public goods with specific uptake mechanisms[17,18], inhibiting competitors[19–21], population demography[22–24] and spatial structuring[10,25–27]. Although in some circumstances cheats can benefit the population[3,28,29], more often they are detrimental to population growth rates, biomass and virulence[2,4,13–15,30,31].

Despite adaptations by producers to limit the loss of the public goods they generate[2,4,14,32–34], a fail-safe alternative exists in nature to achieve this: microbes can internalize substrates before they are metabolized so that all generated products are retained as private goods[35–38]. Given that this strategy overcomes the drawbacks of social exploitation and loss of products, it is surprising that many microbes from diverse taxa still acquire nutrients by producing public goods rather than private goods[1,7,8]. What benefits does it provide?

Here we use the term 'private good' to refer to an extracellular product that is internalized for digestion, as opposed to being digested externally. For example, the corn pathogen *Ustilago maydis* possesses a highly specific and high-affinity sucrose transporter for importing sucrose for private internal breakdown[35], making the sucrose they metabolize a private good. This is in contrast to the rice pathogen *Magnaporthe oryzae*, which feeds on sucrose externally by generating a public good, invertase[3]. Our terminology thus differs from those used in a number of other studies; namely, public-good production can be promoted by linking its expression with so-called 'private goods' that serve a different function, for instance coregulating extracellular proteases with intracellular nucleoside hydrolase[39] or by altering the localization of gene products that serve multiple functions, such as pyoverdine[40]. In addition, the terms 'privatizing' or 'personalizing' have been used to describe gaining a disproportional amount of a public good[41,42]. Furthermore, receptor-specific public goods have been described as 'private goods'[17]. However, such 'private goods' do not overcome the evolutionary incentive for cheating[43], as is the case with our definition.

We assess the benefits of public-goods metabolism using a combination of mathematical modelling and synthetic ecology. We focus on different strategies that *Saccharomyces cerevisiae* deploys to metabolize disaccharides as an ideal exemplar. *S. cerevisiae* can metabolize the disaccharides maltose and sucrose, which have the same molecular formula ($C_{12}H_{22}O_{11}$) but differ in their constituent monosaccharides: maltose consists of two glucose molecules whereas sucrose is one glucose and one fructose molecule. Disaccharides are broken down into their constituent monosaccharides before being catabolized by the glycolytic pathway. Curiously, considering the similarities, *S. cerevisiae* deploys different strategies for their consumption. Maltose is internalized through maltose transporters before being hydrolysed by maltase, whereas sucrose is hydrolysed externally by an extracellular invertase, and the resulting monosaccharides are subsequently internalized[44].

By comparing features of wild-type public sucrose metabolism and private maltose metabolism when grown alone (axenically), we demonstrate how public and private metabolism by *S. cerevisiae* can provide different environment-dependent selective benefits. A number of important differences emerge. Growth on maltose was less hampered by diminishing resource concentrations than growth on sucrose. However, sucrose metabolism facilitated a higher growth rate than maltose metabolism when population density and resource concentrations were sufficiently high.

Biosciences, University of Exeter, Exeter, UK. *e-mail: i.gudelj@exeter.ac.uk

To understand how ecological interactions between such contrasting metabolic strategies influence their evolutionary potential, we deployed a synthetically engineered system consisting of three strains with differing strategies for metabolizing a single resource, sucrose: a public-metabolizer, a private-metabolizer and a cheat. The public-metabolizer is a wild-type strain that generates a public good by secreting invertase, which catalyses the external digestion of sucrose. The private-metabolizer keeps sucrose digestion entirely personal by producing a non-secreted invertase and expressing a high-affinity sucrose transporter protein from *U. maydis*. Finally, the cheat is an invertase gene deletion strain that selfishly exploits the products generated by public-metabolizers, without paying the associated metabolic costs.

Similar to the features of the native private maltose versus public sucrose metabolism, we found that growth of our synthetic private-metabolizer was less hampered at low densities than growth of the public-metabolizer. In addition, private-metabolizers should not suffer from product loss and the subsequent social exploitation experienced by public-metabolizers. When ecological interactions between competing strategies were assessed in long-term communities, we found that public-metabolizers and cheats maintained a stable coexistence. When private-metabolizers were introduced, they gained a selective advantage over other competing strategies to exclude them from the population. However, by combining mathematical models and ecological experiments we discovered a surprising result that could explain why public metabolism is still prevalent amongst microbes. Although the private-metabolizer outcompeted the other competitors, under certain conditions it caused the decline of the entire population. The superior competitive ability was counteracted by a reduced axenic growth rate that, when combined with bottlenecks that can influence interaction outcomes in microbial populations[45–47], led to private metabolism becoming unsustainable.

Results

Opposing native feeding strategies. *S. cerevisiae* metabolizes sucrose externally. A consequence of external metabolism is the loss of the majority of its products into the environment[12,14]. This can prevent populations from successfully establishing[10] or cause low growth rates[11] when population density or resource concentrations are low. This is because public metabolism relies on the collective action of the population to break down substrates to acquire energy-generating nutrients (monosaccharides in this case). Publicly metabolizing cells therefore acquire less nutrients from other individuals at low population density than at high population density and have lower product breakdown rates at low resource concentrations.

First, we considered whether private metabolism, such as that of maltose, would overcome the previously mentioned drawbacks. We found this to be the case when comparing the early growth phase of wild-type *S. cerevisiae* (strain CEN.PK2-1C) on either sucrose or maltose. Unlike public sucrose metabolism, private maltose metabolism did not suffer density-dependent growth rate restrictions (Supplementary Fig. 1), allowing more rapid growth at low population densities than public sucrose metabolism (Fig. 1a and Supplementary Fig. 1a,b). In addition, growth rates on maltose were less hampered by diminishing resource concentrations than growth rates on sucrose, with private maltose metabolism giving rise to faster growth than public sucrose metabolism at low resource concentrations (Fig. 1b and Supplementary Fig. 2). Conversely, public sucrose metabolism facilitated a higher growth rate than private maltose metabolism in high population densities (Fig. 1a and Supplementary Fig. 1a,b) or high resource concentrations (Fig. 1b and Supplementary Fig. 2). Private and public metabolism may therefore represent differing strategies for maximizing growth rates in different environmental circumstances.

In addition to low growth rates associated with public metabolism when resource concentration or population density is low (Fig. 1a,b), the extracellular metabolic products can also be exploited by other individuals that share the environment and hence limit the success of this strategy[3,13,14]. We therefore asked how public and private metabolism would fare when exploitation is possible in mixed-strategy populations. To address this, we used a synthetic experimental system with *S. cerevisiae* strains deploying different strategies for metabolizing a single resource, sucrose.

Public metabolism. In our system, the wild-type strain DBY1034 (here referred to as public-metabolizer) secretes invertase SUC2, which externally hydrolyses sucrose[44]. Invertase is secreted into the environment and is also anchored to the periplasm[48,49]. The extracellular products, glucose and fructose, are publicly available[13,14]. The *SUC2* deletion strain, DBY1701 (here referred to as cheat), does not produce invertase but exploits glucose and fructose in the environment (Fig. 2a).

Extracellular invertase of *S. cerevisiae* is widely considered an exploitable cooperative trait[13,14,22,28,31] and the advantage that public-goods cheats obtain can drive a decline of public-goods producers[2–5,13–15]. Since the public-metabolizer and cheat strains used here have a different genetic background from those classically used to study SUC2 public-goods cooperation[13,14,28], we first verified that they displayed similar features. As observed previously[13,14,28], we confirmed that (1) secreted invertase significantly increased the growth rate of public-metabolizers on sucrose media compared to cheats (Fig. 2b,c), while such differences were not observed on glucose (Supplementary Fig. 3); (2) growth rates of our public-metabolizer were density-dependent (Fig. 2d and Supplementary Fig. 4); and (3) our cheat strain was able to exploit the products of the public-metabolizer to gain a fitness advantage when rarer in the population, with negative frequency-dependent selection enabling public-metabolizers to coexist with cheats (Fig. 2e).

Exploitation by cheats and low growth rates at low population density thus demonstrate the drawbacks of public metabolism and limitations to the success of this feeding strategy.

Private metabolism. In addition to external invertase, *S. cerevisiae* also produces invertase from the *SUC2* gene, which lacks a signal peptide and so remains intracellular[50]. The internal and external forms of invertase have similar catalytic properties[51,52]. To compare the competitive ability of private metabolism with respect to public metabolism, we used a *SUC2* secretion-defective strain (DBY2617), which only produces the internal form of invertase[53]. Some *S. cerevisiae* strains can take up sucrose through maltose transporters[54,55]; however, *S. cerevisiae* primarily feeds by external hydrolysis of sucrose[53] and the S288C genetic background of the strains in this synthetic community are maltose-negative[56]. Into this *SUC2* secretion-defective strain we therefore introduced a specific and high-affinity sucrose transporter *SRT1* from *U. maydis*[35]. SRT1 has more than a 100-fold higher affinity for sucrose than maltose transporters of *S. cerevisiae* and has the capacity to permit rapid growth by providing a carbon source for energy production and metabolism[35,54]. When introduced, the sucrose transporter protein doubled the axenic growth rate of our strain (Supplementary Fig. 5). From here, we refer to this strain as the 'private-metabolizer' (Fig. 2a).

When grown alone in sucrose, the private-metabolizer grew at an intermediate growth rate compared to the public-metabolizer and cheat (Fig. 2b,c), while such differences were not observed on glucose (Supplementary Fig. 3). It does not experience product loss because it metabolizes sucrose internally and, therefore, it does not experience the same extent of density-dependent growth rate as the public-metabolizer. This means that despite having a lower growth rate than the public-metabolizer at higher population density, the private-metabolizer had a higher growth rate than

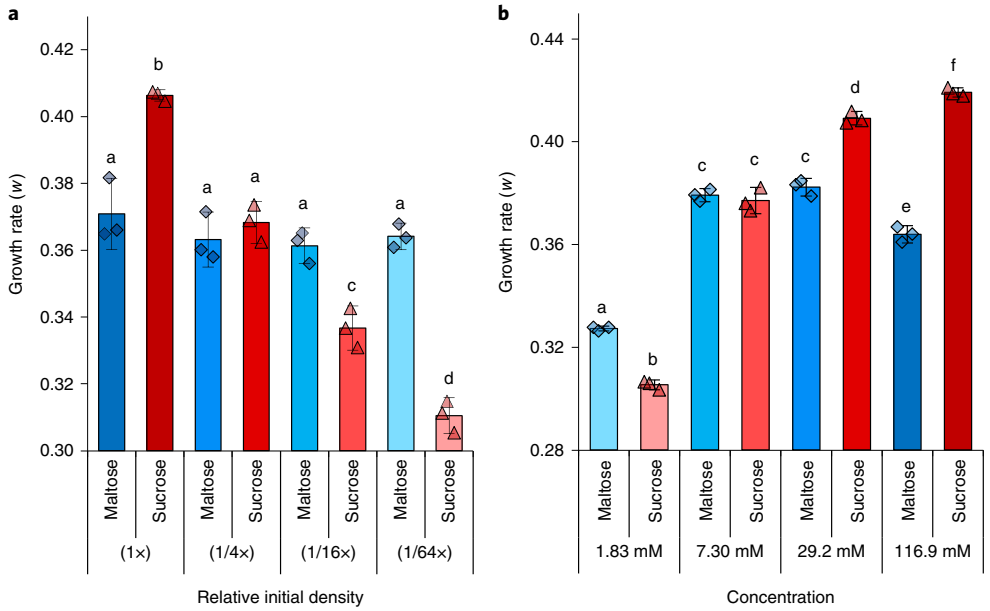

Fig. 1 | Growth rates on privately metabolized maltose or publicly metabolized sucrose with respect to cell and resource concentration. a, Private maltose metabolism enabled faster growth than public sucrose metabolism at lower population density, whereas public sucrose metabolism enabled faster growth in higher population density (Tukey multiple comparison of means: different letters above bars indicate significant differences, $P<0.05$). For equal densities: (1×) $P<2.63\times10^{-5}$, (1/4×) $P=0.951$, (1/16×) $P<1.62\times10^{-3}$, (1/64×) $P<10^{-6}$). All rates in **a** are measured in 29.2 mM sugar. **b**, External public metabolism was also influenced to a greater extent by diminishing resource concentrations (GLM, concentration:sugar interaction term: $F_{(1,\,20)}=14.9$, $P<9.81\times10^{-4}$). Consequently, although public sucrose metabolism enabled faster growth when resource concentrations were sufficiently high (Tukey multiple comparison of means: for equal concentrations, 116.9 mM and 29.2 mM: $P<10^{-7}$), private maltose metabolism was quicker at lower concentration (1.83 mM: $P<6\times10^{7}$). Different letters above bars indicate significant differences ($P<0.05$). All rates in **b** measure from 1× initial density and 1× is approximately 500 c.f.u. μl^{-1}. See Supplementary Figs. 1 and 2 for full datasets; colours are linked to growth curves. Bars show mean ± 95% confidence interval (CI), $n=3$; triangles (sucrose) and diamonds (maltose) show all replicates with added horizontal noise to aid visualization. Data are from the maltose-positive strain CEN.PK2-1C.

the public-metabolizer at low population densities (Fig. 2d and Supplementary Fig. 4). Importantly, the axenic growth features of our engineered system of private and public sucrose metabolizers were in qualitative agreement with the native system of strategies for feeding on internal privately metabolized maltose and external publicly metabolized sucrose (Fig. 1 and Supplementary Fig. 1). This suggests that the comparative growth features of our synthetic system (Fig. 2) were not artefacts of the metabolic engineering of these strains.

We next asked if the private-metabolizer could successfully exclude cheats in mixed populations. We found that over a range of initial frequencies the private-metabolizer had a fitness advantage over cheats, suggesting that cheats would be excluded from the population in the long term (Fig. 2f). Internalizing sucrose metabolism therefore appears to be a successful method of preventing the loss of products from sucrose hydrolysis, both into the environment and to neighbouring cells.

Could the private-metabolizer also outcompete the public-metabolizer? The cheat had an advantage over the public-metabolizer when initially rare (Fig. 2e) because of the cost of invertase production and the metabolic rate-efficiency trade-off[14,28]. However, the private-metabolizer still incurs the cost of producing cytoplasmic invertase[53], in addition to producing the sucrose transporter protein and conducting the energy-dependent transport of sucrose[35]. Despite these costs, we found that the private-metabolizer could outcompete the public-metabolizer over a range of initial frequencies, suggesting that the public-metabolizer would be excluded from the population (Fig. 2g). The superior competitive ability of the private-metabolizer comes from not suffering low growth rate at low density, as the public-metabolizer does (Fig. 2d), but also because it is able to exploit the glucose and fructose from sucrose hydrolysis catalysed by the public-metabolizer.

Long-term community interactions. Short-term pairwise competitions conducted over 24 h (one season) suggested that privatizing sucrose metabolism could be an effective strategy to overcome exploitation and loss of products from public metabolism of sucrose (Fig. 2f–g). We next asked whether these findings are of relevance during long-term community interactions where evolutionary and population dynamics interact. Such interactions are important when predicting the fate of microbial populations[31,57,58].

To address this, we developed a mathematical model that tracked the status of the nutritional environment and the growth of the individual strains within the community during competition in long-term seasonal environments. Mirroring serial transfer experiments, at the end of each 24-h season a fixed proportion of the community was transferred into replenished growth medium. This is equivalent to introducing a mortality rate and mimics the types of natural bottlenecks that microbes experience following disturbances and colonization. Communities were initiated with a majority of public-metabolizers and a minority of other strains to mimic invasion events of novel phenotypes against the ancestral public-metabolizer.

In agreement with the short-term pairwise competitions (Fig. 2f–g), our model predicted that the private-metabolizer would also dominate over the public-metabolizer in the long term when cheats were absent (Fig. 3a) and present (Fig. 3b) in the community. However, our model made a stark prediction about the fate of populations that had become dominated by private-metabolizers: such populations could be destined for decline and eventually become extinct (Fig. 3a,b). In contrast, a community consisting of

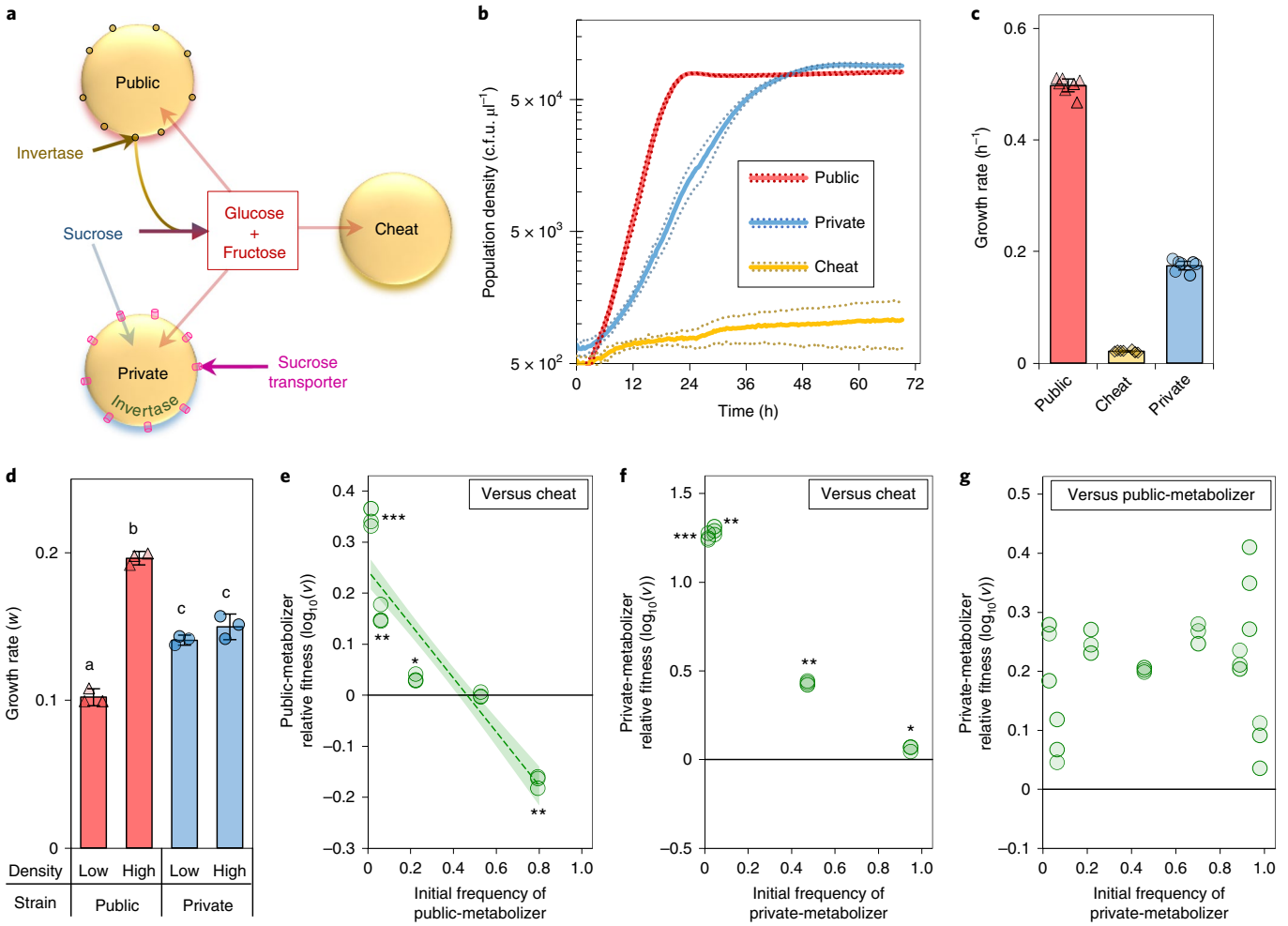

Fig. 2 | Single season growth and pairwise competitiveness of differing sucrose metabolic strategies. a, Schematic of how differing sucrose-use strategies compete for resources. All strains use glucose + fructose released from the public-metabolizer's invertase-mediated external hydrolysis of sucrose. The private-metabolizer can directly import and consume sucrose. **b**, Growth of public-metabolizer, cheat and private-metabolizer strains in monoculture. Solid line shows the mean ± 95% CI (dotted line), $n = 7$. **c**, Between-strain growth rates were significantly different (one-way analysis of variance: $F_{(2, 18)} = 3{,}597.5$, $P < 2.2 \times 10^{-16}$, with post-hoc Tukey ($P < 0.0001$)). Bars show mean ± 95% CI, $n = 7$, markers show all points. The growth rate differences were alleviated on glucose (Supplementary Fig. 3). **d**, The public-metabolizer experienced density-dependent growth rates, whereas the private-metabolizer did not. Letters indicate significant differences (one-way analysis of variance: $F_{(3, 8)} = 162.85$, $P < 1.65 \times 10^{-7}$, with post-hoc Tukey ($P < 0.0001$, non-significant: $P > 0.224$). Mean ± 95% CI, $n = 3$, markers show all points. **e**, Pairwise competitions between public-metabolizers and cheats showed negative frequency-dependent fitness (linear model: $P < 2.78 \times 10^{-6}$, $F_{(1, 13)} = 61.53$, β (± s.e.m.) = −0.527 ± 0.067, Adjusted $r^2 = 0.812$, dashed line ± s.e.m.) with public-metabolizers superior at low initial frequencies (0.015–0.223, one-sample two-sided t-test at each frequency, $t > 7.96$, $^{*}P < 1.54 \times 10^{-2}$, $^{**}P < 4.44 \times 10^{-3}$, $^{***}P < 8.63 \times 10^{-4}$) and inferior at high frequency (0.794, $^{**}P < 1.66 \times 10^{-3}$, $t = 24.6$). Relative fitness was not significantly different at intermediate frequencies (0.527, $P > 0.888$). **f**, In pairwise competition, private-metabolizers outcompeted cheats (one-sample two-sided t-test at each frequency, $t > 7.50$, $^{***}P < 8.18 \times 10^{-5}$, $^{**}P < 1.75 \times 10^{-4}$, $^{*}P < 1.73 \times 10^{-2}$). **g**, In pairwise competition, private-metabolizers outcompeted public-metabolizers ($t = 11.1$, $P < 1.02 \times 10^{-10}$; relative fitness was not frequency-dependent (linear model: $P > 0.471$, $F_{(1, 22)} = 0.5357$) and frequencies were pooled). **e**–**g**, Each initial frequency was tested in triplicate. Relative fitness ($\log_{10}(v)$) was equal at 0.

public-metabolizers and cheats, in the absence of private-metabolizers, could be maintained in the long term (Fig. 3c). Our model suggested that this happens because private-metabolizers have a lower axenic growth rate than public-metabolizers and so take longer to reach high densities (Fig. 2b,c). Communities capable of supporting public-metabolizers (Fig. 3c) could therefore keep up with the mortality rate imposed by population bottlenecks, whereas communities that did not sustain public-metabolizers could not (Fig. 3a,b).

We experimentally tested the model predictions using our three-strain community with batch culture competitions involving serial transfer between seasons. We monitored the strain frequencies and total population density at the end of each 24-h period and found that, as our model predicted, the private-metabolizer dominated the three-strain community (Fig. 3d). When the private-metabolizer reached sufficiently high frequencies the population densities declined sharply (Fig. 3d,e). In contrast, communities containing sufficiently high frequencies of public-metabolizers maintained high densities (Fig. 3d,f) and therefore avoided decline (Fig. 3g). We estimated that saturating population densities of the three-strain community declined once the frequency of private-/public-metabolizers exceeded or fell below certain thresholds (Fig. 3e,f). These thresholds were passed during season 12 and 13, respectively, in Fig. 3d.

Despite finding qualitatively equivalent growth differences between public and private metabolism in the wild-type (Fig. 1) and synthetic strains (Fig. 2b,c), we also tested if the low relative growth rate of the private-metabolizer was caused by features of this specific,

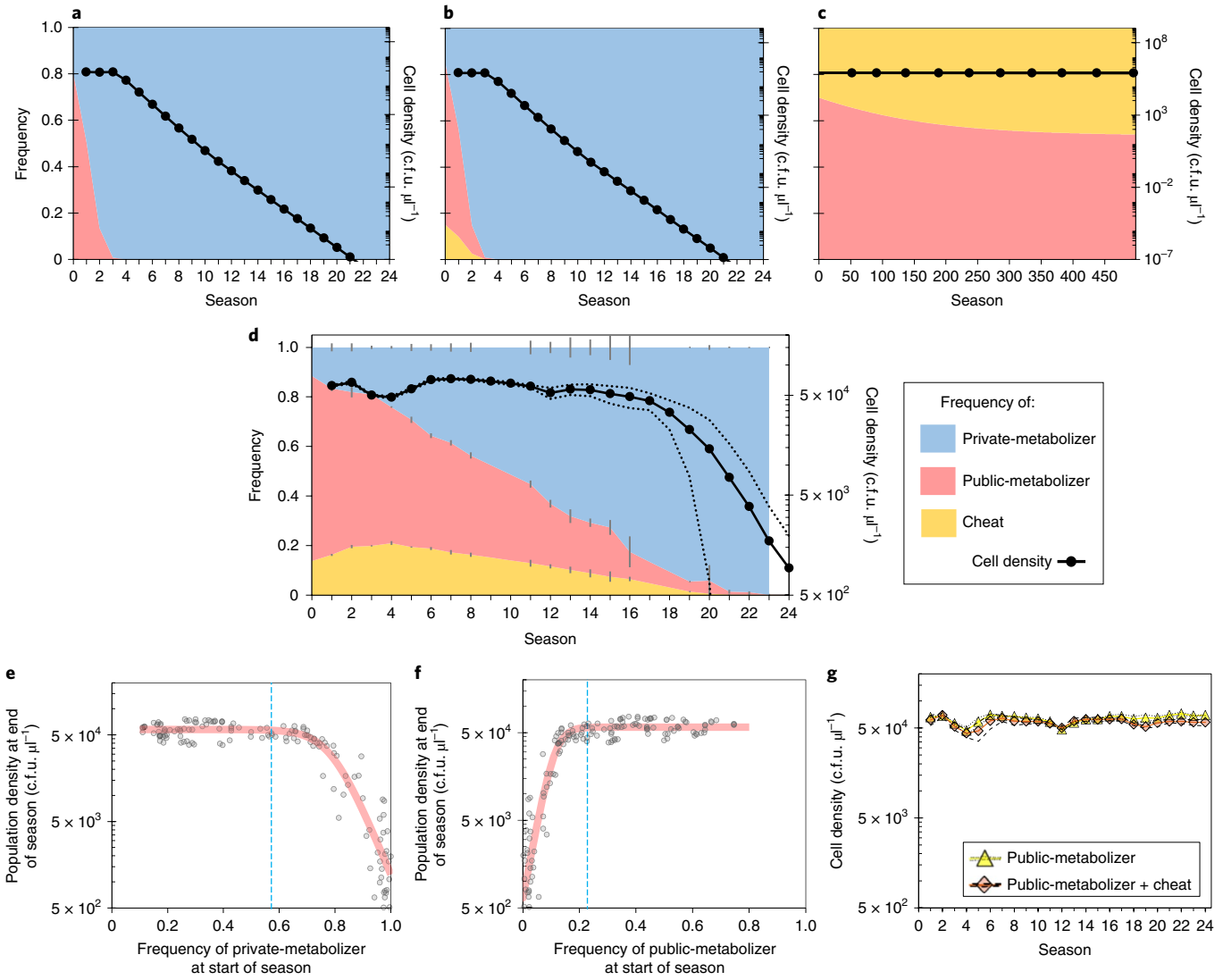

Fig. 3 | Competitiveness and long-term dynamics of sucrose-use polymorphisms. a,**b**, Model simulations predicted that private-metabolizers would dominate in pairwise competitions between public- and private-metabolizers (**a**) and in three-strain communities including cheats (**b**). However, the total cell density declined because of a diminished growth rate. Plots show frequency of strains (left vertical axis) and total cell density (right vertical axis). **c**, Simulations with mixed populations of public-metabolizers and cheats suggested that cheats would initially increase in frequency and then stabilize, but total cell densities continued to reach approximately saturating levels in the long term (>500 seasons). **d**, Experimental test of model with long-term communities, monitoring strain frequencies and total cell density of populations at the end of each season, before transferring 1/150 of the population to fresh media for the subsequent season (mean ± 95% CI, $n = 3$). **e**,**f**, The population density at the end of each season depends on the frequency of private-metabolizers (**e**) and public-metabolizers (**f**) at the beginning of that season. The markers in **e**,**f** show the densities and frequencies from all replicates and seasons of all three-strain communities from **d** and Fig. 4a,b. Solid lines show inverse logistic (**e**, $r^2 = 0.8982$) and logistic equation fit (**f**, $r^2 = 0.8979$). Population decline is instigated once the frequency of private- and public-metabolizers pass estimated thresholds based on the fitted models (>0.572 for private (**e**), <0.228 for public (**f**)), as indicated by blue-dashed line (see Methods for details). **g**, Populations of public-metabolizers, with or without cheats, were able to stably maintain high densities at the end of each season over the course of the serial transfer regimen (mean (solid line and markers) ± 95% CI (dotted line), $n = 3$).

synthetically engineered transport system. First, we tested if the private-metabolizers could be limited by low expression of the sucrose transporter gene which, in turn, limits their sucrose supply leading to a diminished axenic growth rate. Rather than the sucrose transporter gene *SRT1* being regulated by the *PMA1* promoter, we generated a strain where the *SRT1* gene was regulated by the *GPD* promoter, which substantially increased expression of downstream genes (Supplementary Fig. 6). However, this did not significantly change the growth rate of the private-metabolizer (Supplementary Fig. 5b,c), suggesting that the lower growth rate of the private-metabolizer is not limited by low *SRT1* expression.

Second, we asked if resource availability may be limiting the relative growth rate of the private-metabolizer. By examining growth rates of the public- and private-metabolizers over a range of sucrose concentrations, we found that public metabolism of sucrose consistently enabled higher growth rates (Supplementary Fig. 7a,b).

Third, we asked if the low relative growth rate of the private-metabolizer was caused by erroneous heterologous gene expression. We tested this by assessing the growth rates of the private-metabolizer with a *S. cerevisiae* transporter protein. Rather than expressing *U. maydis SRT1*, this strain expressed the *S. cerevisiae* α-glucoside transporter *AGT1* (also known as *Mal11*), which can

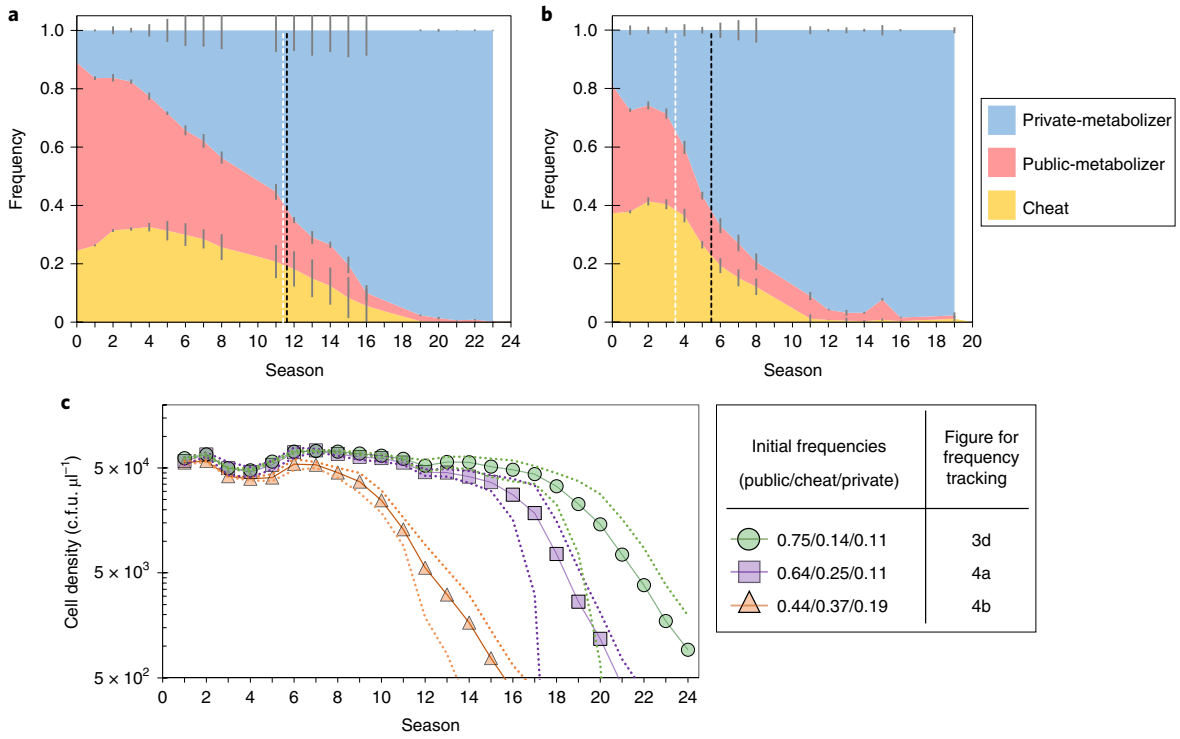

Fig. 4 | Initial strain frequencies determine the timing of population decline in this transfer regimen. a-**c**, Populations initiated with a lower frequency of public-metabolizers and/or a higher frequency of private-metabolizers decline sooner. Three-strain communities were propagated in the same serial transfer regimen as Fig. 3d (0.75/0.14/0.11, public/cheat/private), but with a lower frequency of public-metabolizer (0.64/0.25/0.11) (**a**) and a higher frequency of private-metabolizer (0.44/0.37/0.19) (**b**). The threshold frequencies of private- (black dotted vertical line, mode of three replicates) and public-metabolizers (white dotted vertical line, mode of three replicates) associated with population decline, as estimated in Fig. 3e,f, were reached sooner in these populations, which accelerated the decline of the global population (mean ± 95% CI, $n = 3$) (**c**).Threshold frequencies of public-metabolizers and private-metabolizers were strongly associated with the timing of population decline ($P < 10^{-3}$, Supplementary Fig. 8).

transport sucrose in addition to other disaccharides[55]. Strains in this genetic background do not otherwise express this transporter[56]. Although homologous expression of *AGT1* (by the *PMA1* promoter) enhanced private-metabolizer growth rates compared to *SRT1* expression, it was still inferior to the public-metabolizer rate (Supplementary Fig. 7c). Increased expression with the *GPD* promoter even had a detrimental effect on growth rate (Supplementary Fig. 7c). Collectively, these results suggest that private metabolism is hampered by lower growth rates in a range of nutrient conditions using various uptake systems.

We next postulated that initiating our three-strain communities with higher frequencies of private-metabolizers and/or lower frequencies of public-metabolizers than were used in Fig. 3d would accelerate the observed global population decline. This is because the communities would achieve the required threshold frequencies of private- and public-metabolizers (Fig. 3e,f) sooner than under the starting frequencies deployed in Fig. 3d, causing the population to decline earlier. This is precisely what we observed (Fig. 4). Private-metabolizers became dominant earlier in populations, and public-metabolizers became rarer earlier in populations (Fig. 4a,b). This predictably coincided with the decline of the population (Fig. 4c and Supplementary Fig. 8), thereby confirming that the composition of metabolic strategies within the population determines its fate.

Our long-term community competition studies revealed that populations containing private-metabolizers declined (Fig. 4c), whereas those capable of sustaining public-metabolizers persisted (Fig. 3g) for a 24-h season length and a fixed dilution factor (150×). Next, we examined the resilience of the metabolic strategies for varying dilution factors and season lengths. These factors modify the severity and frequency of bottlenecks that microbial populations may experience. We tested the resilience of single strain populations because private-metabolizers outcompeted public-metabolizers throughout the 24-h season in pairwise competition (Supplementary Fig. 9). During serial transfer regimes, it was found that populations of public-metabolizers persisted for dilution factors much larger than those that could sustain private-metabolizers (Fig. 5a,b). Based on axenic growth characteristics, equivalent resilience predictions were also made with varying season lengths, whereby private-metabolizers were predicted to require much longer seasons to be sustained (44.3 h ± 1.37, mean ± 95% CI) than public-metabolizers (22.6 h ± 0.38) (Supplementary Fig. 10). Despite the drawbacks of product loss, public metabolism can therefore adeptly maintain microbial populations in conditions where private metabolism is unsustainable.

Discussion

Comparisons of the growth characteristics between our synthetic public and private sucrose metabolizers gave qualitatively equivalent results to the comparisons of the growth characteristics between the scenarios of the wild-type metabolizing sucrose publicly and maltose privately (Figs. 1 and 2b,c). As such, the observed growth differences between private and public sucrose metabolizers do not appear to be artefacts exclusive to our engineered strains, but rather they represent more general features of opposing metabolic strategies. In our synthetic community, *S. cerevisiae* strains have the same genetic background and differ only in the way they metabolize sucrose. This allowed us to uniquely probe the benefits and shortcomings of a feeding strategy that relies on private rather than

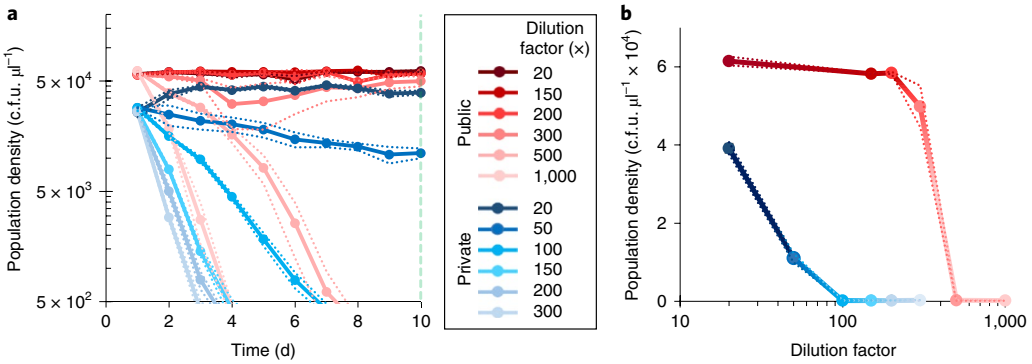

Fig. 5 | Relative resilience of opposing metabolic strategies. a,**b**, The dilution factors implemented between seasons were varied to test the resilience of the different metabolic strategies with respect to the severity of the population bottleneck. Different dilution factors were tested with population density recorded at the end of each ten seasons (**a**). Markers and solid lines show mean, dotted lines show ± 95% CI (often obscured by mean), $n = 3$. Public metabolism (red shades) could sustain high population density with at least 300× dilution, whereas private-metabolizers (blue shades) could only sustain populations with 20× dilution. Densities at the end of season ten are shown in **b** (markers and solid lines shows the mean, dotted lines show ± 95% CI (often obscured by the mean), $n = 3$).

public goods for securing nutrients, while considering interactions between population and evolutionary dynamics. In theory, private strategists should have a clear advantage over those that produce public goods to externally metabolize complex resource because public goods can be lost.

Indeed, we found that keeping metabolism 'private' by directly importing undigested resources into the cell allows individuals to overcome slow growth at low population densities, a drawback that is otherwise experienced by public-metabolizers (Fig. 2d and Supplementary Fig. 4). Populations of public-metabolizers experience an Allee effect, where the per capita growth rate is lower at low densities[11,12]. Due to the cooperative nature of public metabolism, much of the products of sucrose hydrolysis are lost before they can be consumed by the cell that generated them[14]. Many of the products consumed by individual cells are therefore generated by other individuals. At low population density, the probability of acquiring resources generated by others is diminished compared with higher population densities[11], and so the per capita growth rate is lower at low densities. In contrast, keeping metabolism private overcomes the Allee effect. In this case, all the hydrolysis products are retained by the cell that generated them, enabling the cells to grow faster at low population density than those engaging in public metabolism (Figs. 1a and 2c and Supplementary Figs. 1 and 4).

However, at sufficiently high densities, private-metabolizers experience a lower growth rate than public-metabolizers (Figs. 1c and 2c and Supplementary Fig. 1 and 4). The slow growth of the private-metabolizer can be attributed to a combination of factors associated with this feeding strategy. First, the resource uptake capacity of tested disaccharide transporters from a range of organisms are substantially lower than that of hexose transporters[35,55,59–63], even when considering that it effectively transports two monosaccharides simultaneously. Second, the transport of sucrose is frequently an energy-dependent process[35,60,62], whereas glucose transport is an energy-independent process down a concentration gradient[64,65]. In transient environments that microbes frequently inhabit, public metabolism could therefore be a beneficial metabolic strategy by enhancing resource capture. Support for this idea also comes from an unrelated system whereby public metabolism with secreted iron-scavenging siderophores by marine bacteria may accelerate iron uptake. In this case, iron in the environment is predominantly found in the form of slowly diffusing large particles that restrict 'private' uptake rates. Secreted siderophores, however, bind to iron to form small complexes that have increased diffusion and so accelerate iron uptake into the cell[66].

Our study highlights that the combination of a superior competitive ability, relative to both public-metabolizers and cheats, and slow axenic growth rate can put private metabolism at a disadvantage in certain environments. Private-metabolizers are capable of eliminating public-metabolizers from the population, but their slow growth ultimately leads to population decline when alone (Fig. 3a,b,d). In contrast, cheats do not cause populations of public-metabolizers to decline (Fig. 3c,g), despite having a substantially lower growth rate than private-metabolizers (Fig. 2b,c). This is because cheats are less competitive than private-metabolizers, and so they are not capable of sufficiently lowering the frequency of public-metabolizers within the community, which is essential for causing population decline (Figs. 2e and 3f).

We reason that the feeding strategies involving either public or private metabolism represent two opposing approaches to survival, the success of which is environment dependent. Our study suggests that private metabolism may succeed in more stable, non-transient environments, where its lesser growth rate would not hamper the population density it could achieve because the carrying capacity of populations of private-metabolizers is higher than that of public-metabolizers (Fig. 2b). For example, sucrose is privately metabolized by *U. maydis*, a biotrophic fungal pathogen that requires live plant tissue for successful proliferation and so it ensures a prolonged association with its host where it can acquire a steady supply of nutrients[35].

Private metabolism may also succeed in conditions with high microbial genotypic diversity, making public-good production risky due to increased opportunity for exploitation by unrelated individuals. For example, the human gut bacteria *Bacteroides thetaiotaomicron* limits external digestion by transporting oligosaccharides through outer membrane transport proteins into the periplasm where depolymerizing enzymes break them down into the component mono- or disaccharides[36,37]. This metabolic strategy may be particularly profitable when sharing an environment, such as the human intestine, with a multitude of diverse competitor microbes.

Moreover, private metabolism can evolve to be upregulated in response to the emergence of social cheats within genetically diverse microbial communities that are found in cystic fibrosis lung infections[67]. In contrast, we argue that *S. cerevisiae* does not conditionally combine private and public sucrose metabolic strategies to effectively counteract the disadvantages of public metabolism. In particular, as well as secreting invertase, the maltose-positive *S. cerevisiae* strain that was examined for native metabolism (CEN.PK2-1C) (Fig. 1) may import sucrose by expressing the *AGT1* transporter, which may then be broken down by internal invertase[50,55,56]. However, when

growth comparisons between private maltose metabolism and public sucrose metabolism were conducted, the deficiencies associated with public metabolism compared to private maltose metabolism were still evident (Fig. 1).

Finally, private metabolism could thrive in conditions of low population density, such as marine habitats or newly colonized resources. This is because private-metabolizers do not experience the same density-dependent growth rate as public-metabolizers, which results from the loss of secreted products (Figs. 1a and 2d)[10–12]. For instance, marine bacteria exist in relatively low population densities with high diffusion conditions that would be expected to impose an Allee effect for public-metabolizers. As a potential adaptation to overcome this, the marine bacterium *Gramella forsetii* prevents diffusive loss of metabolites by having a 'selfish' uptake mechanism for large oligosaccharides[38].

In contrast, despite the loss of products to neighbours and the environment, public metabolism can be preferential for high growth rate[66,68], such as in transient environments[11] or if a long-term association with a resource is not as crucial. For instance, the rice pathogen *M. oryzae* feeds on sucrose by secreting invertase and its infection cycle is complete in about 1 week[3], whereas the corn pathogen *U. maydis* feeds on sucrose internally and has a longer infection cycle lasting closer to 2 weeks[35,69]. Rapid growth can be crucial to survive population bottlenecks in the long term (Fig. 3d,g). For instance, pathogens experience strong bottlenecks when transmitting to new hosts. Rapid growth may therefore be especially beneficial in short-lived hosts when a high infective dose promotes successful infection[70,71]. Moreover, in environments such as ripe fruit where microbial communities compete fiercely for readily available resources, rapid consumption by public metabolism may be advantageous, especially if exploitation can be prevented. For example, invertase-producing *S. cerevisiae* can protect its public goods by generating an alcoholic and acidic environment, which is toxic to many competitors[20,72].

As public metabolism is widespread, our study suggests that ephemeral environments, where rapid proliferation is necessary to retain a viable long-term population, are frequent in nature. Cheats may undermine their absolute fitness, but mechanisms including frequency-dependence[2,14,23], preferential access[14,22,25–27] and linked private benefits[39,40] can prevent public-metabolizers from becoming extinct. Despite product loss, if public metabolism enables the fastest way of acquiring nutrients, as demonstrated (Figs. 1c,d and 2b–d) and theoretically predicted[66,68], then it can provide a distinct advantage over private metabolism. Although private metabolism in such ephemeral environments can provide a competitive edge over cooperative public metabolism, it can ultimately lead to population decline and increasing its vulnerability to extinction.

Methods

Strains. Strains were supplied by the Boles lab (Goethe University), the Botstein lab (Princeton University) and the Fink lab (Whitehead Institute). CEN.PK2-1C was used to compare wild-type strategies for public sucrose metabolism and private maltose metabolism because it is maltose-positive, unlike strains in the S288C genetic background[56]. In the synthetic community, DBY1034 (ref. [53]) was used as a wild-type secreted invertase (*SUC2*, GenBank: CAA24618.1, UniProt: D5MS22) producing wild-type strain of *S. cerevisiae* (referred to as 'public-metabolizer'), a segregant from the ninth backcross of a series of backcrosses to introduce the *ura3-52* marker from Francois Lacroute strains into the S288c background (Professor Marian Carlson, Columbia University, personal communication, 20 November 2014). The invertase non-producing strain, DBY1701, was used as a 'cheat' strain[53]. The 'private-metabolizer' strain was generated by modification of DBY2617, which possesses a signal sequence mutation *suc2-438* resulting in a deletion from amino acid 4-19, so that the invertase produced is retained within the cytoplasm[53]. A sucrose transporter gene (*SRT1*) from the plant pathogenic fungus *U. maydis* was introduced to DBY2617 (ref. [35]). Similar to a strain generated previously to characterize *SRT1*, constitutive expression was regulated by the plasma membrane ATPase gene (*PMA1*) promoter[60]. However, to ensure that the gene was a single copy and it was maintained, rather than the gene residing on the NEV-E plasmid[35,60], we introduced the gene construct chromosomally at the *URA3* locus using the integrating plasmid pRS306, linearized with *EcoRV*[73]. This modification significantly increased the growth rate (Supplementary Fig. 5). The *AGT1* constructs were also generated in pRS306, linearized with *EcoRV*[73].

To maintain identical auxotrophic requirements and so that strains could be distinguished in mixed populations (Supplementary Fig. 11), the public-metabolizer expressed *eYFP* by the *TEF1* promoter and the cheat expressed *mCherry* by the *TEF1* promoter, both introduced into the *URA3* locus with pRS306 linearized with *EcoRV*, whereas the private-metabolizer was untagged. These fluorescent markers had no detectable fitness effects in otherwise isogenic strains (Supplementary Fig. 12). The resulting strains were all *MATa his4-539 lys2-801*.

Media, growth assays and competitions. *S. cerevisiae* strain CEN.PK2-1C was grown in 6.9 g l^{-1} yeast nitrogen base without amino acids, 790 mg l^{-1} complete supplement mixture (Formedium) with maltose or sucrose (Fisher Scientific) at the specified concentrations. Starter cultures were inoculated in 1% (w/v) of the sugar that the strain was subsequently cultured in. *S. cerevisiae* strains for the synthetic communities were grown in 5 g l^{-1} ammonium sulfate (Fisher Scientific), 1.7 g l^{-1} yeast nitrogen base without amino acids and ammonium sulfate (BD Difco), 20 mg l^{-1} L-histidine, 50 mg l^{-1} L-lysine (Sigma Aldrich) with 1% (w/v) glucose (for starter cultures and experiment in Supplementary Fig. 4) and 1% (w/v) sucrose for growth assays and competitions (Fisher Scientific). All media was filter sterilized (0.2 µm) to prevent breakdown and remove particulate matter that may cause noise during flow cytometry.

Starter cultures were grown in 5 ml media shaken at 180 r.p.m. overnight at 30 °C. Cells were washed and resuspended in fresh media to a density of 5×10^2 colony-forming units (c.f.u.) µl^{-1}, established using a spectrophotometer calibrated to known densities. From these cultures, lower initial density populations were appropriately diluted with media.

Experiments were performed in 48-well suspension culture plates (640 µl per well) (Greiner Bio-One). Cultures were incubated at 30 °C with maximum orbital shaking in a microplate reader (FLUOstar Omega (BMG) at 700 r.p.m. for CEN.PK2-1C; Spark 10 M (Tecan) at 500 r.p.m. for other strains. All direct comparisons were made from the same microplate reader). Each well was considered a replicate. Population density was measured by optical density $(OD)_{620\,nm}$ readings. OD was converted to cell density (c.f.u.) using a calibration of known densities (Supplementary Fig. 13)[22]. This measure could accurately determine cell densities over approximately 1×10^3 c.f.u. µl^{-1}.

Growth rates (r) in Fig. 2c and Supplementary Figs. 3b and 5c were estimated as described previously[74], except they used c.f.u. instead of OD to measure population density (N) from growth data using the logistic equation:

$$\frac{dN}{dt} = rN\left(1 - \frac{N}{K}\right) \quad (1)$$

whose solutions are modified to account for lag phase, where $\frac{dN}{dt}$ is the microbial per capita growth rate and r and K (carrying capacity) are calculated from the best fit to density time series of:

$$N(t) = \frac{K}{1 + \exp^{-r(t-L)}} \quad (2)$$

where $N(t)$ is density at time t and L is lag and denotes the time taken to reach the mid-point of the sigmoid.

Correlation coefficients (r^2) shown for model fits (Fig. 3e,f) represent least squares regression. Parameter estimates to determine threshold frequencies of strains that led to population decline were based on $1-2L$ (Fig. 3e) or $2L$ (Fig. 3f) from the modified logistic equation described above.

For conditions where growth was measured from low starting density that could not be detected in the plate reader, or when resource concentration was sufficiently low/high (Figs. 1 and 2c and Supplementary Figs. 1 and 2), growth rates were determined using Malthusian growth parameters (w)[75]:

$$w = \frac{\left(\frac{N(\text{final})}{N(\text{initial})}\right)}{t} \quad (3)$$

where N(initial) is the initial population density and N(final) is the population density at time t (h). In Fig. 1 and Supplementary Figs. 1 and 2, N(final) is the population density for the first measurement of the time series that the population density exceeds 1.6×10^4 c.f.u. µl^{-1} (at least five doublings for the highest initial density). In Fig. 2 and Supplementary Fig. 4, N(final) is the final density measured. As discussed in ref. [75], this measure incorporates both features of lag phase and growth rate, which varies between differing metabolic strategies.

To test for the Allee effect in the synthetic community (Supplementary Fig. 4), cells were inoculated into 10 ml sucrose media and incubated at 30 °C with 180 r.p.m. orbital shaking because cell densities were too low to be measured accurately by OD. Density was measured hourly by flow cytometry by extracting 250 µl of the population.

Relative fitness of strains (v) was established by monitoring changes in frequency[23]:

$$v = \frac{x_2(1 - x_1)}{x_1(1 - x_2)} \quad (4)$$

where x_1 and x_2 are the initial and final frequency of the focal strain, respectively.

Competition experiments were initiated by mixing individual strains (5×10^2 c.f.u. μl^{-1} in sucrose media) at volumetric frequencies, with precise initial frequencies measured by flow cytometry. Growth proceeded for 24 h (except for data in Supplementary Fig. 9), after which cell populations were diluted to determine the final frequency of strains by flow cytometry. For long-term competitions, 1/150 (or various dilutions in Fig. 5) of the population was transferred to fresh media for subsequent growth seasons. For populations that had reached an approximate stationary phase, this dilution returned cell density to approximately equal to the starting density at day 0 (5×10^2 c.f.u. μl^{-1}). Communities were assumed to be destined for extinction when the density at the end of the season did not exceed the initial density at the start of day 0 (5×10^2 c.f.u. μl^{-1}). Flow cytometry was performed using a Guava easyCyte 10HT System using Guava InCyte software (Merck Millipore). Frequencies were determined by gating events on forward scatter (FSC) and side scatter (SSC) and strains distinguished by fluorescence protein properties (Supplementary Fig. 11).

Mathematical model. Here we adapt and simplify the system-specific model developed by us in ref. [28] to track in time the concentrations of sucrose (S) and hexose (H) in the environment, as well as the densities of the three-strain community involving public-metabolizers (P), private-metabolizers (T) and cheats (C). We assume that all strains take up resources R and use them to generate ATP using a simple, unbranched pathway[76]. The rate of ATP production in the pathway is denoted by J^{ATP} and is given by $J^{ATP}=n^R_{ATP}J^R$, where J^R denotes the rate of the pathway, which is a function of resource concentration R. The term n^R_{ATP} denotes the number of ATP molecules produced in the pathway. In practice, yield of ATP production is not as easy to measure as the efficiency, n^R_e whereby $n^R_e=bn^R_{ATP}$, with b denoting the constant amount of biomass formed per unit of ATP. We also represent microbial growth as a linear function of the rate of ATP production[28,76,77], namely rJ^{ATP}, where r is some proportionality constant, which here we set to 1.

Public-metabolizers produce invertase, an enzyme that catalyses the extracellular hydrolysis of each molecule of sucrose into two hexose molecules (H). The rate of conversion of sucrose into hexose is represented by Inv, a saturating function of sucrose concentration and taking the following from:

$$Inv(S)=r_{in}\frac{S}{S+k_{in}} \tag{5}$$

where r_{in} denotes invertase activity, which for simplicity is assumed to be constant, as in ref. [14], while k_{in} denotes a saturation constant.

The cost of invertase secretion is denoted by a constant c, estimated empirically in ref. [28]. To reflect this in our model, we multiply the fitness of public-metabolizers by $(1-c)$, as in refs. [14,28]. Following ref. [28], we assume that the activity of the secreted invertase is immediate and it does not accumulate in time. It also does not diffuse because it is predominantly anchored to the cell wall[44,50].

Private-metabolizers also produce invertase in order to hydrolyse sucrose, although the invertase produced is a 'private good' andso not communally accessible[53]. Its production incurs energetic cost c_l.

All three strains transport hexose molecules into the cell by hexose transporters and the rate of the hexose pathway J^H is defined by:

$$J^H=\frac{V^H_{max}H}{K^H+H} \tag{6}$$

where V^H_{max} denotes the maximal rate of the pathway and K^H denotes the respective Michaelis–Menten constant. The efficiency of this pathway is denoted by n^H_e.

Sucrose molecules are hydrolysed in close proximity of public-metabolizers and therefore these cells have preferential access to the hexose they liberate from sucrose[14]. We represent this phenomenon by assuming that the K^H in equation (6) is lower for public-metabolizers (denoted by K^H_p) than the other strains (K^H_n).

S. cerevisiae metabolism is frequently constrained by a rate-efficiency trade-off, where an increase in resource uptake rate leads to a decrease in the biomass created per gram of resource[59,78–80]. We also find evidence for this trade-off in our system where public-metabolizers cultured in isolation grow quicker but to lower final density (carrying capacity) than private-metabolizers, which grow slower but to higher final density (Fig. 2b and Supplementary Fig. 14a,b). We therefore assume that the efficiency of hexose uptake n^H_e is a decreasing function of hexose available in the environment.

Private-metabolizers take up sucrose through the highly specific and high-affinity sucrose transporter *SRT1* (ref. [35]) before they metabolize it internally, converting it into simpler sugars and eventually into molecules of ATP. The rate of that sucrose pathway is defined by:

$$J^S=\frac{V^S_{max}S}{K^S+S} \tag{7}$$

where V^S_{max} denotes the maximal rate of the pathway and K^S denotes the respective Michaelis–Menten constant. The efficiency of that pathway is denoted by a constant n^S_e. Although public-metabolizers and cheats may be able to inefficiently take up sucrose through maltose transporters[54], it is not specifically included in the model because the same pathway exists for the otherwise isogenic private-metabolizers.

The system dynamics. Taking into account the above assumptions and considering a well-mixed environment where the concentrations of sucrose, hexose, public-metabolizers, private-metabolizers and cheats do not depend on spatial location we arrive at the following Ordinary Differential Equation model:

$$\begin{aligned}\frac{dS}{dt}&=-InvP-J^ST\\ \frac{dH}{dt}&=(2Inv-J^H)P-J^HT-J^HC\\ \frac{dP}{dt}&=(1-c)n^H_eJ^HP\\ \frac{dT}{dt}&=(1-c_l)(n^H_eJ^H+n^S_eJ^S)T\\ \frac{dC}{dt}&=n^H_eJ^HC\end{aligned} \tag{8}$$

We consider the following initial conditions:

$$\begin{aligned}S(0)=S_0,H(0)=0,P(0)=f^P_0N_0,\\ T(0)=f^T_0N_0,C(0)=f^C_0N_0\end{aligned} \tag{9}$$

where N_0 is the total initial population density and f^P_0, f^T_0, f^C_0 are the initial frequencies of public-metabolizers, private-metabolizers and cheats respectively, where $f^P_0+f^T_0+f^C_0=1$.

The long-term competition outcome between the three strains is determined in the following way. The Ordinary Differential Equation model (equation (2)) is run for a fixed time (a 'season'), and we calculate the final frequencies of each strain $f^P_{end}, f^T_{end}, f^C_{end}$ and the final population density N_{end} at the end of each season. The subsequent growth season is initiated with the following initial conditions:

$$\begin{aligned}S(0)=S_0,H(0)=0,P(0)=f^P_{end}N_{end}/D,\\ T(0)=f^T_{end}N_{end}/D,C(0)=f^C_{end}N_{end}/D\end{aligned} \tag{10}$$

where D is the dilution factor. We repeat this procedure over a number of seasons and track how the final population density and frequencies of each strain changes over time. This procedure mimics the serial transfer experimental design.

Parameters. The parameter values are listed in Supplementary Table 1. In particular, parameters c and k_{in} are taken from ref. [28]. The other parameters $V^H_{max}, K^H_p, r_{in}, V^S_{max}, K^S$ and n^S_e have been fitted to the growth curves of public- and private-metabolizers grown axenically in sucrose media (Supplementary Fig. 14a). The hexose rate-efficiency trade-off[78,79] is assumed to be of the form shown (Supplementary Fig. 14c). The value of K^H_n was chosen such that it allows for coexistence of public-metabolizers and cheats as predicted experimentally (Fig. 2e).

Data analysis. Statistical tests and data analysis were performed using R v.3.4.1. and Excel 2013/2016. The parameters associated with the logistic equation were estimated by fitting the equation to growth data using Solver Add-in.

Pairwise comparisons were performed with two-sample two-sided t-tests. Welch's two-sample two-sided t-tests were used when variance was found to be unequal (by two-sample F-test for variances). Multiple comparisons were made with general linear models (GLMs) with post-hoc Tukey multi-comparison of means (honest significant differences method). GLMs were used to analyse density-, resource- or strain-dependence of growth rates (dependent variables) (Supplementary Figs. 1b,d,f, 2d, 5 and 7b) and, when applicable, to test for interactions between the explanatory variables: (1) 'carbon source' and 'density' (Fig. 1a, Supplementary Fig. 1f), (2) 'carbon source' and $\log_{10}$ 'concentration' (Fig. 1b), (3) between 'strain' and 'carbon source' (Supplementary Fig. 3) and (4) between 'strain' and exp('time') terms (Supplementary Fig. 4). GLMs had these terms as explanatory variables (main effects) with a two-way interaction between them. Frequency-dependent fitness was tested with a linear model and relative fitness differences were measured by one-sample t-tests. Models were assessed with quantile–quantile plots of standardized residuals and plotting model-fitted values against standardized residuals to check assumptions of normality and homoscedasticity, respectively.

Correlation was tested by least squares regression analysis (Fig. 3e,f) and Spearman's correlation analysis (Supplementary Fig. 8).

Reporting Summary. Further information on research design is available in the Nature Research Reporting Summary linked to this article.

Data availability

The research data supporting this publication can be found at https://doi.org/10.24378/exe.1383.

Received: 12 April 2018; Accepted: 12 June 2019;
Published online: 22 July 2019

References

1. Richards, T. A. & Talbot, N. J. Horizontal gene transfer in osmotrophs: playing with public goods. *Nat. Rev. Microbiol.* **11**, 720–727 (2013).
2. Drescher, K., Nadell, C. D., Stone, H. A., Wingreen, N. S. & Bassler, B. L. Solutions to the public goods dilemma in bacterial biofilms. *Curr. Biol.* **24**, 50–55 (2014).

3. Lindsay, R. J., Kershaw, M. J., Pawlowska, B. J., Talbot, N. J. & Gudelj, I. Harbouring public good mutants within a pathogen population can increase both fitness and virulence. *eLife* **5**, e18678 (2016).
4. Bachmann, H., Molenaar, D., Kleerebezem, M. & van Hylckama Vlieg, J. E. High local substrate availability stabilizes a cooperative trait. *ISME J.* **5**, 929–932 (2010).
5. Griffin, A. S., West, S. A. & Buckling, A. Cooperation and competition in pathogenic bacteria. *Nature* **430**, 1024–1027 (2004).
6. Chang, Q. et al. A unique invertase is important for sugar absorption of an obligate biotrophic pathogen during infection. *New Phytol.* **215**, 1548–1561 (2017).
7. Lincoln, L. & More, S. S. Bacterial invertases: occurrence, production, biochemical characterization, and significance of transfructosylation. *J. Basic Microbiol.* **57**, 803–813 (2017).
8. Parrent, J. L., James, T. Y., Vasaitis, R. & Taylor, A. F. Friend or foe? Evolutionary history of glycoside hydrolase family 32 genes encoding for sucrolytic activity in fungi and its implications for plant–fungal symbioses. *BMC Evol. Biol.* **9**, 148 (2009).
9. Voegele, R. T., Wirsel, S., Möll, U., Lechner, M. & Mendgen, K. Cloning and characterization of a novel invertase from the obligate biotroph *Uromyces fabae* and analysis of expression patterns of host and pathogen invertases in the course of infection. *Mol. Plant Microbe Interact.* **19**, 625–634 (2006).
10. Koschwanez, J. H., Foster, K. R. & Murray, A. W. Improved use of a public good selects for the evolution of undifferentiated multicellularity. *eLife* **2**, e00367 (2013).
11. Dai, L., Vorselen, D., Korolev, K. S. & Gore, J. Generic indicators for loss of resilience before a tipping point leading to population collapse. *Science* **336**, 1175–1177 (2012).
12. Völker, C. & Wolf-Gladrow, D. A. Physical limits on iron uptake mediated by siderophores or surface reductases. *Mar. Chem.* **65**, 227–244 (1999).
13. Greig, D. & Travisano, M. The Prisoner's Dilemma and polymorphism in yeast *SUC* genes. *Proc. Biol. Sci.* **271**(Suppl. 3), S25–S26 (2004).
14. Gore, J., Youk, H. & van Oudenaarden, A. Snowdrift game dynamics and facultative cheating in yeast. *Nature* **459**, 253–256 (2009).
15. Harrison, F., Browning, L. E., Vos, M. & Buckling, A. Cooperation and virulence in acute *Pseudomonas aeruginosa* infections. *BMC Biol.* **4**, 21 (2006).
16. Kümmerli, R., Schiessl, K. T., Waldvogel, T., McNeill, K. & Ackermann, M. Habitat structure and the evolution of diffusible siderophores in bacteria. *Ecol. Lett.* **17**, 1536–1544 (2014).
17. Niehus, R., Picot, A., Oliveira, N. M., Mitri, S. & Foster, K. R. The evolution of siderophore production as a competitive trait. *Evolution* **71**, 1443–1455 (2017).
18. Lee, W., Van Baalen, M. & Jansen, V. A. An evolutionary mechanism for diversity in siderophore-producing bacteria. *Ecol. Lett.* **15**, 119–125 (2012).
19. Riley, M. A. & Wertz, J. E. Bacteriocins: evolution, ecology, and application. *Annu Rev. Microbiol.* **56**, 117–137 (2002).
20. Celiker, H. & Gore, J. Competition between species can stabilize public-goods cooperation within a species. *Mol. Syst. Biol.* **8**, 621 (2012).
21. Verstrepen, K. J. et al. Glucose and sucrose: hazardous fast-food for industrial yeast? *Trends Biotechnol.* **22**, 531–537 (2004).
22. Lindsay, R. J., Pawlowska, B. J. & Gudelj, I. When increasing population density can promote the evolution of metabolic cooperation. *ISME J.* **12**, 849–859 (2018).
23. Ross-Gillespie, A., Gardner, A., West, S. A. & Griffin, A. S. Frequency dependence and cooperation: theory and a test with bacteria. *Am. Nat.* **170**, 331–342 (2007).
24. Ross-Gillespie, A., Gardner, A., Buckling, A., West, S. A. & Griffin, A. S. Density dependence and cooperation: theory and a test with bacteria. *Evolution* **63**, 2315–2325 (2009).
25. Kümmerli, R., Griffin, A. S., West, S. A., Buckling, A. & Harrison, F. Viscous medium promotes cooperation in the pathogenic bacterium *Pseudomonas aeruginosa*. *Proc. Biol. Sci.* **276**, 3531–3538 (2009).
26. Allison, S. D. Cheaters, diffusion and nutrients constrain decomposition by microbial enzymes in spatially structured environments. *Ecol. Lett.* **8**, 626–635 (2005).
27. Julou, T. et al. Cell–cell contacts confine public goods diffusion inside *Pseudomonas aeruginosa* clonal microcolonies. *Proc. Natl Acad. Sci. USA* **110**, 12577–12582 (2013).
28. MacLean, R. C., Fuentes-Hernandez, A., Greig, D., Hurst, L. D. & Gudelj, I. A mixture of 'cheats' and 'co-operators' can enable maximal group benefit. *PLoS Biol.* **8**, e1000486 (2010).
29. Driscoll, W. W., Pepper, J. W., Pierson, L. S. & Pierson, E. A. Spontaneous Gac mutants of *Pseudomonas* biological control strains: cheaters or mutualists? *Appl. Environ. Microbiol.* **77**, 7227–7235 (2011).
30. Rainey, P. B. & Rainey, K. Evolution of cooperation and conflict in experimental bacterial populations. *Nature* **425**, 72 (2003).
31. Sanchez, A. & Gore, J. Feedback between population and evolutionary dynamics determines the fate of social microbial populations. *PLoS Biol.* **11**, e1001547 (2013).
32. Rakoff-Nahoum, S., Foster, K. R. & Comstock, L. E. The evolution of cooperation within the gut microbiota. *Nature* **533**, 255–259 (2016).
33. Galeote, V. et al. *FSY1*, a horizontally transferred gene in the *Saccharomyces cerevisiae* EC1118 wine yeast strain, encodes a high-affinity fructose/H^+ symporter. *Microbiology* **156**, 3754–3761 (2010).
34. Brown, C. J., Todd, K. M. & Rosenzweig, R. F. Multiple duplications of yeast hexose transport genes in response to selection in a glucose-limited environment. *Mol. Biol. Evol.* **15**, 931–942 (1998).
35. Wahl, R., Wippel, K., Goos, S., Kämper, J. & Sauer, N. A novel high-affinity sucrose transporter is required for virulence of the plant pathogen *Ustilago maydis*. *PLoS Biol.* **8**, e1000303 (2010).
36. Cuskin, F. et al. Human gut Bacteroidetes can utilize yeast mannan through a selfish mechanism. *Nature* **517**, 165–169 (2015).
37. Martens, E. C., Koropatkin, N. M., Smith, T. J. & Gordon, J. I. Complex glycan catabolism by the human gut microbiota: the Bacteroidetes Sus-like paradigm. *J. Biol. Chem.* **284**, 24673–24677 (2009).
38. Reintjes, G., Arnosti, C., Fuchs, B. M. & Amann, R. An alternative polysaccharide uptake mechanism of marine bacteria. *ISME J.* **11**, 1640 (2017).
39. Dandekar, A. A., Chugani, S. & Greenberg, E. P. Bacterial quorum sensing and metabolic incentives to cooperate. *Science* **338**, 264–266 (2012).
40. Jin, Z. et al. Conditional privatization of a public siderophore enables *Pseudomonas aeruginosa* to resist cheater invasion. *Nat. Commun.* **9**, 1383 (2018).
41. Zhang, X. X. & Rainey, P. B. Exploring the sociobiology of pyoverdin-producing *Pseudomonas*. *Evolution* **67**, 3161–3174 (2013).
42. Pande, S. et al. Privatization of cooperative benefits stabilizes mutualistic cross-feeding interactions in spatially structured environments. *ISME J.* **10**, 1413 (2016).
43. Inglis, R. F., Biernaskie, J. M., Gardner, A. & Kümmerli, R. Presence of a loner strain maintains cooperation and diversity in well-mixed bacterial communities. *Proc. Biol. Sci.* **283**, https://doi.org/10.1098/rspb.2015.2682 (2016).
44. Schweizer, M. & Dickinson, J. R. *The Metabolism and Molecular Physiology of Saccharomyces cerevisiae* (CRC Press, 2004).
45. Zhou, L., Slamti, L., Nielsen-LeRoux, C., Lereclus, D. & Raymond, B. The social biology of quorum sensing in a naturalistic host pathogen system. *Curr. Biol.* **24**, 2417–2422 (2014).
46. Travisano, M. & Velicer, G. J. Strategies of microbial cheater control. *Trends Microbiol.* **12**, 72–78 (2004).
47. Brockhurst, M. A., Buckling, A. & Gardner, A. Cooperation peaks at intermediate disturbance. *Curr. Biol.* **17**, 761–765 (2007).
48. Rouwenhorst, R. J., Van Der Baan, A. A., Scheffers, W. A. & Van Dijken, J. Production and localization of beta-fructosidase in asynchronous and synchronous chemostat cultures of yeasts. *Appl. Environ. Microbiol.* **57**, 557–562 (1991).
49. Tammi, M., Ballou, L., Taylor, A. & Ballou, C. Effect of glycosylation on yeast invertase oligomer stability. *J. Biol. Chem.* **262**, 4395–4401 (1987).
50. Carlson, M. & Botstein, D. Two differentially regulated mRNAs with different 5′ ends encode secreted and intracellular forms of yeast invertase. *Cell* **28**, 145–154 (1982).
51. Williams, R. S., Trumbly, R. J., MacColl, R., Trimble, R. B. & Maley, F. Comparative properties of amplified external and internal invertase from the yeast SUC2 gene. *J. Biol. Chem.* **260**, 13334–13341 (1985).
52. Gascón, S., Neumann, N. P. & Lampen, J. O. Comparative study of the properties of the purified internal and external invertases from yeast. *J. Biol. Chem.* **243**, 1573–1577 (1968).
53. Kaiser, C. A. & Botstein, D. Secretion-defective mutations in the signal sequence for *Saccharomyces cerevisiae* invertase. *Mol. Cell. Biol.* **6**, 2382–2391 (1986).
54. Stambuk, B. U., Batista, A. S. & De Araujo, P. S. Kinetics of active sucrose transport in *Saccharomyces cerevisiae*. *J. Biosci. Bioeng.* **89**, 212–214 (2000).
55. Stambuk, B. U., da Silva, M. A., Panek, A. D. & de Araujo, P. S. Active α-glucoside transport in *Saccharomyces cerevisiae*. *FEMS Microbiol. Lett.* **170**, 105–110 (1999).
56. Vidgren, V., Ruohonen, L. & Londesborough, J. Characterization and functional analysis of the MAL and MPH loci for maltose utilization in some ale and lager yeast strains. *Appl. Environ. Microbiol.* **71**, 7846–7857 (2005).
57. Lion, S. Theoretical approaches in evolutionary ecology: environmental feedback as a unifying perspective. *Am. Nat.* **191**, 21–44 (2017).
58. McPeek, M. A. The ecological dynamics of natural selection: traits and the coevolution of community structure. *Am. Nat.* **189**, E91–E117 (2017).
59. Otterstedt, K. et al. Switching the mode of metabolism in the yeast *Saccharomyces cerevisiae*. *EMBO Rep.* **5**, 532–537 (2004).
60. Sauer, N. & Stolz, J. SUC1 and SUC2: two sucrose transporters from *Arabidopsis thaliana*; expression and characterization in baker's yeast and identification of the histidine-tagged protein. *Plant J.* **6**, 67–77 (1994).
61. Weise, A. et al. A new subfamily of sucrose transporters, SUT4, with low affinity/high capacity localized in enucleate sieve elements of plants. *Plant Cell* **12**, 1345–1355 (2000).

62. Reinders, A. & Ward, J. M. Functional characterization of the α-glucoside transporter Sut1p from *Schizosaccharomyces pombe*, the first fungal homologue of plant sucrose transporters. *Mol. Microbiol.* **39**, 445–455 (2001).
63. Elbing, K. et al. Role of hexose transport in control of glycolytic flux in *Saccharomyces cerevisiae*. *Appl. Environ. Microbiol.* **70**, 5323–5330 (2004).
64. Bisson, L. F., Coons, D. M., Kruckeberg, A. L. & Lewis, D. A. Yeast sugar transporters. *Crit. Rev. Biochem. Mol. Biol.* **28**, 259–308 (1993).
65. Özcan, S. & Johnston, M. Function and regulation of yeast hexose transporters. *Microbiol. Mol. Biol. Rev.* **63**, 554–569 (1999).
66. Leventhal, G. E., Ackermann, M. & Schiessl, K. T. Why microbes secrete molecules to modify their environment: the case of iron-chelating siderophores. *J. R. Soc. Interface* **16**, 20180674 (2019).
67. Andersen, S. B. et al. Privatisation rescues function following loss of cooperation. *eLife* **7**, e38594 (2018).
68. Vetter, Y., Deming, J., Jumars, P. & Krieger-Brockett, B. A predictive model of bacterial foraging by means of freely released extracellular enzymes. *Microb. Ecol.* **36**, 75–92 (1998).
69. Dean, R. et al. The top 10 fungal pathogens in molecular plant pathology. *Mol. Plant Pathol.* **13**, 414–430 (2012).
70. Kothary, M. H. & Babu, U. S. Infective dose of foodborne pathogens in volunteers: a review. *J. Food Safety* **21**, 49–68 (2001).
71. Schmid-Hempel, P. & Frank, S. A. Pathogenesis, virulence, and infective dose. *PLoS Pathog.* **3**, e147 (2007).
72. Piskur, J., Rozpedowska, E., Polakova, S., Merico, A. & Compagno, C. How did *Saccharomyces* evolve to become a good brewer? *Trends Genet.* **22**, 183–186 (2006).
73. Sikorski, R. S. & Hieter, P. A system of shuttle vectors and yeast host strains designed for efficient manipulation of DNA in *Saccharomyces cerevisiae*. *Genetics* **122**, 19–27 (1989).
74. Reding-Roman, C. et al. The unconstrained evolution of fast and efficient antibiotic-resistant bacterial genomes. *Nat. Ecol. Evol.* **1**, 0050 (2017).
75. Lenski, R. E., Rose, M. R., Simpson, S. C. & Tadler, S. C. Long-term experimental evolution in *Escherichia coli*. I. Adaptation and divergence during 2,000 generations. *Am. Nat.* **138**, 1315–1341 (1991).
76. Pfeiffer, T., Schuster, S. & Bonhoeffer, S. Cooperation and competition in the evolution of ATP-producing pathways. *Science* **292**, 504 (2001).
77. Bauchop, T. & Elsden, S. R. The growth of micro-organisms in relation to their energy supply. *J. Gen. Microbiol.* **23**, 457–469 (1960).
78. Postma, E., Verduyn, C., Scheffers, W. A. & Van Dijken, J. P. Enzymic analysis of the crabtree effect in glucose-limited chemostat cultures of *Saccharomyces cerevisiae*. *Appl Environ. Microbiol* **55**, 468–477 (1989).
79. Weusthuis, R. A., Pronk, J. T., van den Broek, P. J. & van Dijken, J. P. Chemostat cultivation as a tool for studies on sugar transport in yeasts. *Microbiol. Rev.* **58**, 616–630 (1994).
80. Badotti, F. et al. Switching the mode of sucrose utilization by *Saccharomyces cerevisiae*. *Microb. Cell Fact.* **7**, 4 (2008).

Acknowledgements

We thank R. Beardmore, A. Jepson and P. Holder for comments and helpful discussions. R.J.L. and I.G. are funded by European Research Council Consolidator Grant No. 647292 MathModExp awarded to I.G., and B.J.P. was funded by an EPSRC Doctoral training studentship.

Author contributions

R.J.L. and I.G. conceived the idea. R.J.L. and I.G designed the experiments. R.J.L. carried out the experiments. B.J.P. and I.G. developed the mathematical model. B.J.P. carried out numerical simulations. R.J.L. and I.G. analysed the results and wrote the manuscript.

Competing interests

The authors declare no competing interests.

Additional information

Supplementary information is available for this paper at https://doi.org/10.1038/s41559-019-0944-9.

Reprints and permissions information is available at www.nature.com/reprints.

Correspondence and requests for materials should be addressed to I.G.

Publisher's note: Springer Nature remains neutral with regard to jurisdictional claims in published maps and institutional affiliations.

nature research

Corresponding author(s): Ivana Gudelj

Last updated by author(s): May 23, 2019

Reporting Summary

Nature Research wishes to improve the reproducibility of the work that we publish. This form provides structure for consistency and transparency in reporting. For further information on Nature Research policies, see Authors & Referees and the Editorial Policy Checklist.

Statistics

For all statistical analyses, confirm that the following items are present in the figure legend, table legend, main text, or Methods section.

n/a	Confirmed	
☐	☒	The exact sample size (*n*) for each experimental group/condition, given as a discrete number and unit of measurement
☐	☒	A statement on whether measurements were taken from distinct samples or whether the same sample was measured repeatedly
☐	☒	The statistical test(s) used AND whether they are one- or two-sided *Only common tests should be described solely by name; describe more complex techniques in the Methods section.*
☐	☒	A description of all covariates tested
☐	☒	A description of any assumptions or corrections, such as tests of normality and adjustment for multiple comparisons
☐	☒	A full description of the statistical parameters including central tendency (e.g. means) or other basic estimates (e.g. regression coefficient) AND variation (e.g. standard deviation) or associated estimates of uncertainty (e.g. confidence intervals)
☐	☒	For null hypothesis testing, the test statistic (e.g. *F*, *t*, *r*) with confidence intervals, effect sizes, degrees of freedom and *P* value noted *Give P values as exact values whenever suitable.*
☒	☐	For Bayesian analysis, information on the choice of priors and Markov chain Monte Carlo settings
☒	☐	For hierarchical and complex designs, identification of the appropriate level for tests and full reporting of outcomes
☐	☒	Estimates of effect sizes (e.g. Cohen's *d*, Pearson's *r*), indicating how they were calculated

Our web collection on statistics for biologists contains articles on many of the points above.

Software and code

Policy information about availability of computer code

Data collection	Spark 10M microplate reader (Tecan) used SparkControl V2.1 software (Tecan) and FLUOstar Omega (BMG) used Omega V3.00 software (BMG) to control growth conditions and make optical density readings from which population densities were calculated. Guava Easycyte 10HT was controlled using guavaSoft 3.2 and data was extracted using Guava InCyte software 3.2 (Merck Millipore). Simulations of our mathematical model were performed with Matlab's differential equation solvers. Data fitting was performed using non-linear fitting routines from MATLAB Optimisation Toolbox.
Data analysis	R statistical software, version 3.4.1 and Excel 2013/2016.

For manuscripts utilizing custom algorithms or software that are central to the research but not yet described in published literature, software must be made available to editors/reviewers. We strongly encourage code deposition in a community repository (e.g. GitHub). See the Nature Research guidelines for submitting code & software for further information.

Data

Policy information about availability of data

All manuscripts must include a data availability statement. This statement should provide the following information, where applicable:

- Accession codes, unique identifiers, or web links for publicly available datasets
- A list of figures that have associated raw data
- A description of any restrictions on data availability

The research data supporting this publication can be found at https://doi.org/10.24378/exe.1383

Field-specific reporting

Please select the one below that is the best fit for your research. If you are not sure, read the appropriate sections before making your selection.

☒ Life sciences ☐ Behavioural & social sciences ☐ Ecological, evolutionary & environmental sciences

For a reference copy of the document with all sections, see nature.com/documents/nr-reporting-summary-flat.pdf

Life sciences study design

All studies must disclose on these points even when the disclosure is negative.

Sample size	n >= 3 for all experiments, equivalent to comparable published studies. These samples were sufficient to detect significant differences between treatments/strains, or to determine the fate of mixed populations. Performing an a priori power analysis was not appropriate for our study, as we were not seeking to detect pre-specified differences between samples.
Data exclusions	No data was excluded from analyses
Replication	All experiments were performed in at least triplicate. To verify robustness, the main finding of privatisation of public goods causing population collapse was repeated with three different initial strain frequencies (each with n = 3) with equivalent outcomes.
Randomization	Populations were randomly allocated to wells within the 48-well plate. Populations of individual strains were initiated from a random single colony from an agar plate.
Blinding	Investigator was not blind during data collection/analysis because subjective measurements were not made.

Reporting for specific materials, systems and methods

We require information from authors about some types of materials, experimental systems and methods used in many studies. Here, indicate whether each material, system or method listed is relevant to your study. If you are not sure if a list item applies to your research, read the appropriate section before selecting a response.

Materials & experimental systems

n/a	Involved in the study
☒	☐ Antibodies
☒	☐ Eukaryotic cell lines
☒	☐ Palaeontology
☐	☒ Animals and other organisms
☒	☐ Human research participants
☒	☐ Clinical data

Methods

n/a	Involved in the study
☒	☐ ChIP-seq
☐	☒ Flow cytometry
☒	☐ MRI-based neuroimaging

Animals and other organisms

Policy information about studies involving animals; ARRIVE guidelines recommended for reporting animal research

Laboratory animals	This study did not involve laboratory animals
Wild animals	This study did not involve wild animals
Field-collected samples	This study did not involve samples collected from the field
Ethics oversight	No ethical or approval guidance was required because the study involved harmless microorganisms

Note that full information on the approval of the study protocol must also be provided in the manuscript.

Flow Cytometry

Plots

Confirm that:

☒ The axis labels state the marker and fluorochrome used (e.g. CD4-FITC).

☒ The axis scales are clearly visible. Include numbers along axes only for bottom left plot of group (a 'group' is an analysis of identical markers).

☒ All plots are contour plots with outliers or pseudocolor plots.

☒ A numerical value for number of cells or percentage (with statistics) is provided.

Methodology

Sample preparation	Lab strain Saccharomyces cerevisiae cells were cultured overnight in filter sterilized (0.2 micron) media (as defined in methods section) and for flow cytometry the density of the cultured was diluted appropriately in the same media, omitting sugar.
Instrument	Guava Easycyte 10HT (Merck Millipore)
Software	Guava InCyte software 3.2 (Merck Millipore)
Cell population abundance	5000 events were acquired per replicate for all competition experiments and Allee effect measurements. 10,000 events were measured for testing promoter expression of eYFP (Supplementary Figure S6). All reagents for culturing cells for experiments involving flow cytometry were filter sterilized with a 0.2 micron syringe filter (Minisart) to eliminate particulate matter that may compromise the purity of cell measurements. Strains were distinguished based on fluorescent protein properties as detailed in Supplementary Figure S11.
Gating strategy	Cell populations were gated on FSC and SSC to specify S. cerevisiae cells from any other particles. This gated > 95% of detected events which were screened for fluorescent protein properties. NB. This gating procedure was used to determine strain frequencies only. Parallel population density measurements were made by optical density (Supplementary figure S13). Excitation lasers used were green (532 ± 5 nm) for mCherry, and blue (488 ± 5) for eYFP. Emission was detected with green (525/30 nm) for eYFP, and orange (620/52 nm) for mCherry. To distinguish strains in mixed populations, for every time point a single strain population of each genotype was measured for reference. Mixed populations were subsequently measured and events gated to give distinct regions of each strain. Example plots and data of this procedure is detailed in Supplementary Figure S11.

☒ Tick this box to confirm that a figure exemplifying the gating strategy is provided in the Supplementary Information.